Flexible Planet Pins for High Torque Epicyclic Gears: Experience with Design, Manufacturing, and Application

Hanspeter Dinner, Deputy General Manager, KISSsoft AG

For wind turbine main gearboxes (MGBs) with about 1 MW or higher power, gearbox designs with multiple power paths are used. They handle several mega-Newton-meter of torque economically. Earlier wind turbines with lower power ratings used parallel shaft gearboxes with only one power path but soon they were superseded by planetary gearboxes having typically three to five planets per stage. This paper describes experiences using planetary gears where "Flexpins" are used to improve the load sharing between the individual planets—representing the multitude of power paths—and along the planet's face width.

Introduction

Wind Turbines MGB, Cantilevered Plant Pin Support

Technologies with respect to materials (high purity steels for bearings and gears), design (use of elastic structures improve load sharing between gears), bearing design (adjusted roller crowning allowing for higher misalignment, integration of raceway into the planet gear, use of hydrodynamic bearings) and gearbox architecture (increased number of planets, optimal selection of ratio per stage, single-walled planet carriers, compound planetary stages) allow for ever increasing torque density. Below, an example design with two planetary stages in series with a high-speed parallel shaft stage is shown. The LSS features five planets, which still yields a good ratio of maximum i_{LSS}~4.1 (see Table 4 [Ref. 7]). By experience, three, four, and five planets result in good load distribution and sufficiently high ratio. Studies in other industries confirm this. For example, in turboprop engines, reduction gearboxes are used where the goal of maximized torque density at high reliability is the same as for wind turbines. Below Figure 1, bottom, from Ref. 8, shows that a planetary stage, considering bearing and gear life, yields the highest system life over a range up to a ratio 1:4 (for five-planet design) to 1:5 (for three- and four-planet designs).

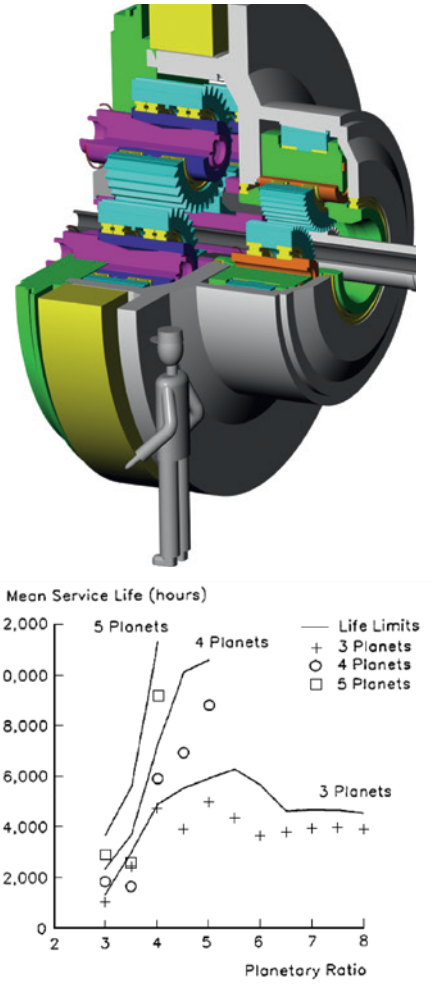

Figure 1—Top: Example 8 MW MGB with five planets, supported on flexible planet pins in LSS and conventional ISS (yellow body represents the turbine main bearing). Bottom: Service life of a planetary stage as a function of ratio and number of planets (Ref. 8).

Designs with a high number of planets face three major design challenges: 1) load sharing among the planets 2) load distribution along the planet's face width 3) space for the carrier. The first two problems are related to the third in that since there is not much space for the carrier, it becomes soft, resulting in a larger misalignment of the planets concerning the sun gear and the ring gear. The solution presented here to tackle all three problems at once is using a single-walled carrier and cantilevered planet pins. The planet pins are of the "Flexpin" type, as invented and patented by Ray Hicks (Ref. 16). Such a design allows for a higher number of planet pins projecting from a flange, while each pin supports a planet gear for orbital rotation about the gearbox axis. No space is required between the planets for the connecting pieces connecting the two flanges of a conventional planet carrier design and planet outer diameters may nearly touch. As a simple rule of thumb use the credit card approach: if you can fit a credit card between the tip diameters, you should be fine. The simple construction of the single-wall carrier accommodates a larger number of planet gears, and hence the planetary stage will handle a proportionately larger torque. The condition is that the tilting of the planets due to the pin bending is managed properly. This paper focuses on "proper management."

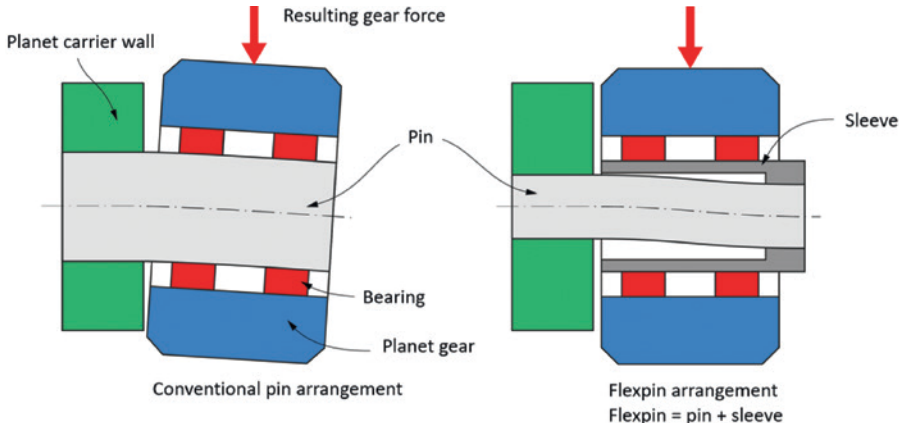

Figure 2—Working principle of the Flexpin arrangement (right). Conventional pin arrangement in single-walled carriers (left). Planet gear (blue) supported in a single-walled carrier (green) does not tilt if Flexpin (grey for the pin and dark grey for the sleeve) is used (right). Planet gear (blue) does tilt if a simple cantilevered pin (grey) is used (left).

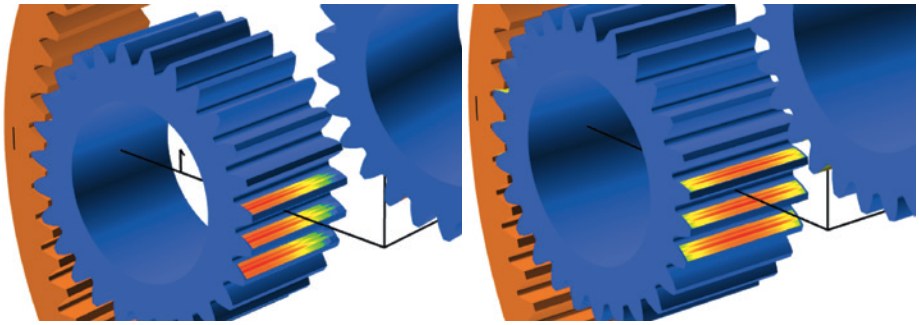

Figure 3—Contact stress distribution on planet tooth in mesh with the sun (not shown). Note gradient (left) and symmetry (right) in contact stress along the face width. Left: Conventional pin arrangement. Right: Flexpin arrangement. Compare to Figure 2 above.

Figure 4–Upscaled carrier design, bearings and planet gears not yet mounted onto the Flexpins. Planets and bearings not yet assembled, for a 6 MW MGB.

Number of Planets and Load Sharing

The basic design problem to solve in planetary gears is to ensure near-equal load sharing among the multitude of planets. A perfect power-split is not achieved and the level of unevenness in the power-split is highly dependent on machining accuracy and system elasticity. The load sharing among the planets gets worse with a higher number of planets, sometimes such that increasing the number of planets does not result in an overall higher power or torque capacity anymore. The load sharing among the planets is expressed by the mesh load factor K_γ in gear design and rating, e.g., along ISO 6336. The mesh load factor or load sharing factor K_γ is defined as $K_\gamma = max(Ti) / average(Ti)$ where Ti is the torque transmitted through each planet or load path. The minimum value of K_γ is $K_{\gamma\_opt} = 1.00$, meaning that each planet takes the same load. Typical K_γ values for planetary gear stages are in the range of 1.10 to 1.25. K_γ is used in the gear rating for all failure modes (e.g., scuffing, micropitting, tooth flank fracture, pitting, bending, etc.). Recommended design values are listed in Ref. 7 and shown below. They tend to be conservative when compared to tests.

A study (Ref. 10), on the combined influence of the number of planets, torque levels, and the carrier pinhole position errors on planet load-sharing and gear root stresses confirmed that a floating three-planet gear set has near-equal load sharing, regardless of the manufacturing error values. It also confirmed that the planet loads and gear stresses are sensitive to the carrier pinhole position errors. Other studies, e.g., Refs. 11–15, confirm the trends and to some extent the numerical values shown above.

Second, to the mesh load factor K_γ, the face load factor $K_{H\beta}$ is considered in the

Application level[1), 4), 5)]		Number of planets, N_{CP}								AGMA accuracy grade[2)]	Flexible mounts[3)]
		2	3	4	5	6	7	8	9		
1	K_γ[6)]	1.16	1.23	1.32	1.35	1.38	1.47	1.60	~	A7 or worse	without
2	K_γ[6)]	1.00[7)]	1.00[7)]	1.25	1.35	1.44	1.47	1.60	1.61	A5–A6	without
3	K_γ[6)]	1.00[7)]	1.00[7)]	1.15	1.19	1.23	1.27	1.30	1.33	A4 or better	without
4	K_γ[6)]	1.00[7)]	1.00[7)]	1.08	1.12	1.16	1.20	1.23	1.26	A4 or better	with

Figure 5—K_γ values for different application levels and gear accuracy grades, with and without Flexpin (right side column labeled "Flexible mounts"), Ref. 7.

gear rating, e.g., along ISO 6336. It describes the evenness of the load distribution along the face width in the mesh between the sun and planet and planet and ring gear. If the load along the face width is evenly distributed, then, $K_{H\beta}$ = 1.00 applies. $K_{H\beta}$ is defined as the maximum value of the line load width, divided by the mean value, $K_{H\beta} = max(w) / average(w)$. Since the Flexpin results in a movement of the planet parallel to the gearbox axis (see Figure 2, right), the load distribution remains symmetric to the planet's face width and hence optimal (see Figure 3, right). The resulting $K_{H\beta}$ are then typically $K_{H\beta}$ = 1.15 and the modifications applied on the planets are only a slight flank line crowning.

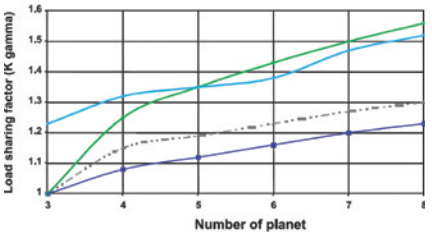

Figure 6—Load sharing factors (blue for measurement with Flexpin) compared to values stipulated in different guidelines. The measurement confirms that the use of a Flexpin allows for a much lower load-sharing factor to be used when compared to general design guidelines (Ref. 10).

Use of Flexpin in Wind Turbine MGBs

The single-wall carrier in combination with the concept of mounting the planet gears on Flexpins gives the design high reliability (because the contact between planet and sun flank and planet and ring gear flank remains near optimal for different torque levels) and high torque capacity (because of the elevated number of planets). Numerous gearbox designs for wind turbine MGBs using Flexpins exist. However, it must be said that the use of the Flexpin concept is not used in high numbers. Most of the leading MGB OEMs companies do not use the Flexpin in their design; this is a strong indicator against the use of the Flexpin for standard gearbox designs. It means that there are probably good reasons not to use Flexpins in a conventional gearbox design and this means that the advantages and disadvantages of the Flexpin design must be carefully considered.

Flexpin Use in SCD Turbine Main Gearboxes

Flexpin as Used in SCD Gearboxes

Figure 8 of Flexpins manufactured by the author shows a similar design. The conical shapes are designed such that an almost constant stress level along the pin axis results, thereby maximizing the utilization of the material or reducing the mass of the pin. The parts shown are hard turned, before machining of the threads for the locknuts and heat treatment. The critical areas of the pin, particularly the fillet radii, are polished to reduce the effect of surface roughness on their strength. Also, pins are nitrided, resulting in a hardened outer layer with very little deformation during the heat treatment process. The hardened layer is thin, less than 1 mm but increases the stress at the surface (where the highest stresses are present) considerably.

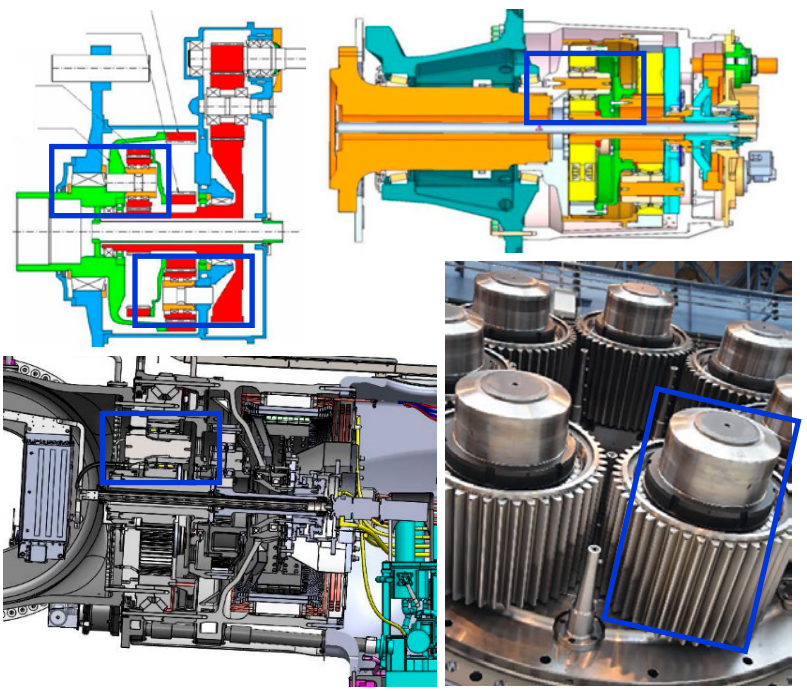

Figure 7—Top left: Gearbox design by MAAG (Ref. 17), believed to be the first wind turbine MGB featuring Flexpins. Top right: Design of a wind turbine MGB using Flexpins, having a compound planetary arrangement (sun gear of second stage connects to the ring gear of first stage (Ref. 19). Bottom left: SCD gearbox designed by the author (Ref. 9). Bottom right: Planetary stage with seven planets, 7 MW wind turbine MGB by WIKOV (Ref. 18). Flexpin highlighted in cross-sectional images.

Figure 8–Flexpin pins, awaiting transport to heat treatment.

The right pin is cooled down and inserted into the sleeve.

Calculation of Load Distribution

The planetary stage having five planets supported on Flexpins is modelled as a combination of springs and gaps. The springs model the stiffness of the parts while gaps are used to model manufacturing errors. Errors considered using gaps included

- Pitch error in the teeth
- Differences in the bearing clearances
- Misalignment between Flexpin pin and sleeve
- Positioning errors of the Flexpin in the carrier

The starting point is the spring model of a planetary stage with five planets as shown below. From the carrier torque and the center distance, a force Ftot is determined that is then distributed—as a function of the spring stiffness values and the gaps (position errors) into the five planets. In the five planets, the five F_1, F_2, F_3, F_4, F_5 are present. They are not exactly the same, K_γ is then K_γ = max(F_1, F_2, F_3, F_4, F_5) / average(F_1, F_2, F_3, F_4, F_5). Each planet is further broken down into a more detailed spring system as shown below.

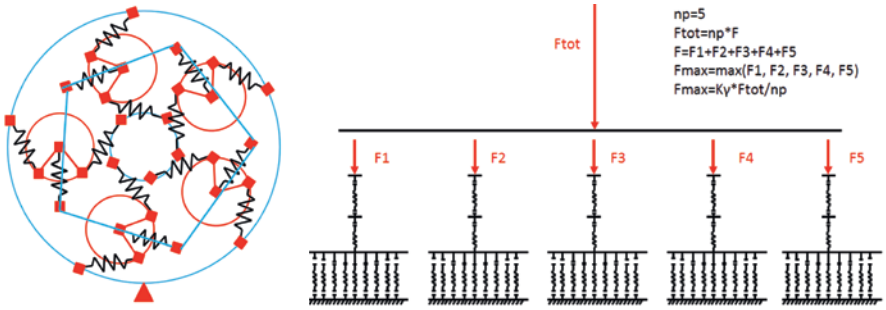

Figure 9—Spring model of a planet stage with five planets. Left: meshes and Flexpins as springs. Right: Corresponding model with gear meshes modeled finely.

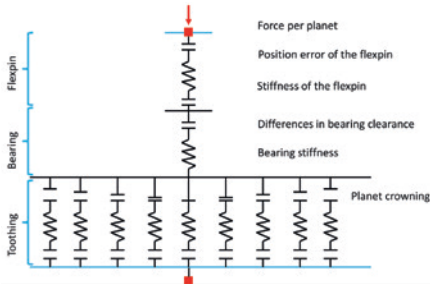

Figure 10—Spring-gap model of one planet. Note the spring representing the Flexpin.

The contacts between ring gear and planet and between sun and planet are represented by one contact. The crowning is considered, it varies over the tooth width. The pitch error is modeled as a gap in the contact between the planet and the sun/ring gear.

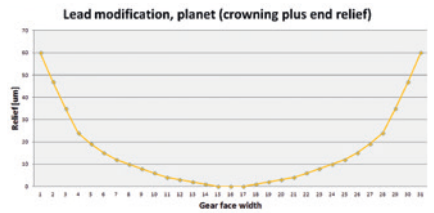

Figure 11—Planet modification combining slight crowning with linear end relief on either side.

For the different errors considered in the model, the following ranges are defined:

- Pitch error of teeth: a gear quality of Q=6 is assumed, resulting in +-20 µm possible pitch error in the mesh. The mesh itself is represented by 31 individual springs to model also a crowning.
- Variation of the bearing clearance: For a bearing with d=320 mm and clearance C3 (305 µm to 225 µm) a variation of ±40 µm is used, this may be conservative.
- Flexpin: Here, two errors are considered. The positioning error (using quality IT6 on the center distance, giving a tolerance of ±80 µm, again somewhat conservative) and the concentricity error (between pin and sleeve, assuming IT5, giving ±50 µm, again somewhat conservative).

These errors were then determined for all five pins using *Microsoft Excel* number generator. A total of 20 random numbers for each of the errors in the five Flexpins were used and added up giving twenty experiments. Within the above-defined range of the errors, a random number / value for the error was used (using *Microsoft Excel* to determine a random number using a constant probability distribution). So, a random error in the bearing clearance variation (variation from bearing to bearing) of 40 µm to +40 µm, a random error in the flex pin position of -80 µm to +80 µm, a random error in the gear pitch of -20 µm to +20 µm and a random error in the concentricity of the Flexpin pin to sleeve of -50 µm to +50 µm was defined. The random errors were then added up to give five total errors for each planet. The procedure was repeated twenty times to give twenty random error distributions for the planetary stage.

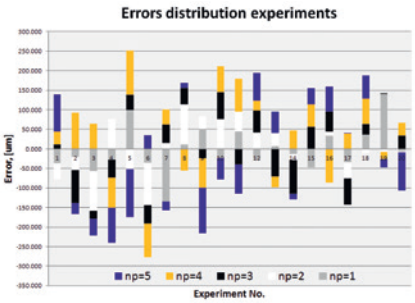

Figure 12—Resulting manufacturing errors for the five planets, shown for 20 random experiments.

Now that the manufacturing errors and gaps in the gear meshes are defined, the force distribution among the five pins may be calculated from the known spring stiffness values. This is done for 20 random manufacturing error groups. From the Flexpin forces F_1, F_2, F_3, F_4, F_5, load distribution factor K_γ may be calculated. The average value is found at K_γ = 1.13 and 95 percent of all values are below K_γ = 1.14.

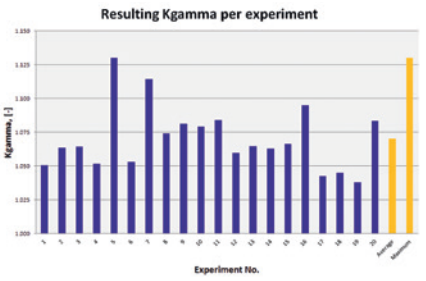

Figure 13—Resulting K_γ for 20 experiments, average and maximum value.

Experimental Measurement of Load Distribution

The SCD drive train was subjected to operating loads and the Flexpin deformation was measured. Measurement over time showed a fluctuation of the load-sharing factor, possibly induced by the heavy masses present in the gearbox that are superimposed to the external torque load. Two types of tests were conducted, one where only torque load was applied and a second test where the torque load was superimposed with a bending moment corresponding to the bending moment as experienced in a typical wind situation. Note that the bending moment has a major influence on the load sharing in this design (see exploded view below) as the gearbox is an integral part of the whole load-bearing structure. Also, in the load path there is the main bearing integrated into the gearbox and any clearance or stiffness of the main bearing contributes to a tilting of the planet carrier and therefore affects the load distribution. This is an effect that was not relevant or not considered in all other studies shown here and the additional results generated in this study are worth mentioning. The resulting load sharing factor K_γ = 1.23 was found, well above the load sharing factor under pure torque only. However, the value found in the measurement confirmed the value used for design at K_γ = 1.25.

Figure 14—Test of the drive train under torque and bending load. Blue part in the background: E-motor to generate the torque load. Yellow part: torque coupling. Grey box with angled top: device to apply bending moments (Ref. 9).

- Max. Displacement / mean Displacement
- Decreasing Kγ with increasing power
- Within expected range for increasing power and no load situations
- Measured Kγ = 1.12, torque load only
- Compare to AGMA 6123-C16, Table 7, Kγ = 1.12

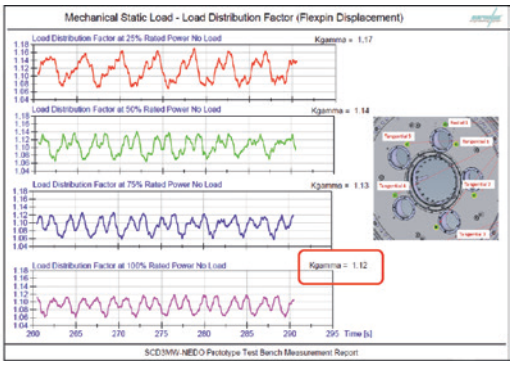

Figure 15—Measurement of load sharing factor (calculated from five measurements of Flexpin deformation), only torque applied, for different torque levels (Ref. 9).

- Added tilt moment at 100 % turbine power
- Situation for continuous added load, in practice high tilt and bending loads occur for a short amount of time
- Measured Kγ = 1.20...1.23, torque load and bending load
- Design value of Kγ = 1.25 confirmed

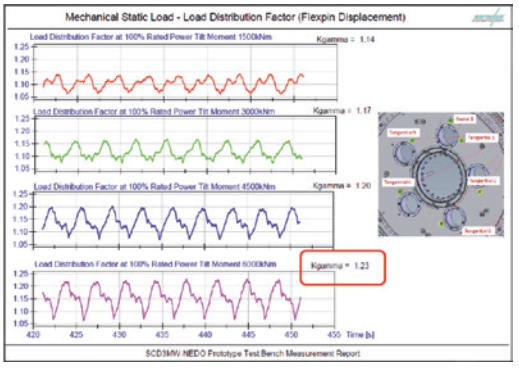

Figure 16—Measurement of load sharing factor (calculated from five measurements of Flexpin deformation) with bending moment applied, for different torque levels (Ref. 9).

Note that the above measured value at K_γ = 1.12 happens to correspond to the value given in AGMA 6123, for five planets, application level 4 with flexible mounts. Application level 4 with flexible mounts is for "high quality, high speed, gas turbine/generator drives, military marine" applications. Wind turbines are classified there as application level 2 in general, there is no specific application level for wind turbines with Flexpins mentioned.

Shape Optimization

Motivation

During the above design, analysis, manufacturing, and testing of the Flexpins, it became apparent that manufacturing costs are largely independent of the pin shape while the load distribution among the planet greatly benefits from a lowered pin stiffness. Optimizing the pin shape to reduce its stiffness while keeping stress levels was attempted to have the best possible design if and when the need for a higher torque main gearbox arises.

Flexpin Pin Shapes Compared

Others have worked on optimized pin shapes earlier. In the study (Ref. 6), five designs are compared.

1. Conventional design / no Flexpin
2. Flexpin with original design by Ray Hicks (see Figure 17, left, for pin shape)
3. Flexpin with circumferential groove (see Figure 17, second from left, for pin shape)
4. Flexpin with spindle shape (see Figure 17, second from right, for pin shape)
5. Flexible conventional planet pin supported on both sides (see right side of Figure 17)

The target in these optimizations is to achieve the lowest stiffness (hence best load sharing among the planets) while not overstressing the pin. While the original Flexpin (Figure 17, left) was strictly cylindrical, the most common design uses a series of several cylinders (second design from left). Montestruc then further improved the design by using two tapered halves. The purpose of the below optimization is to further refine this design to achieve near-constant stress distribution along the pin.

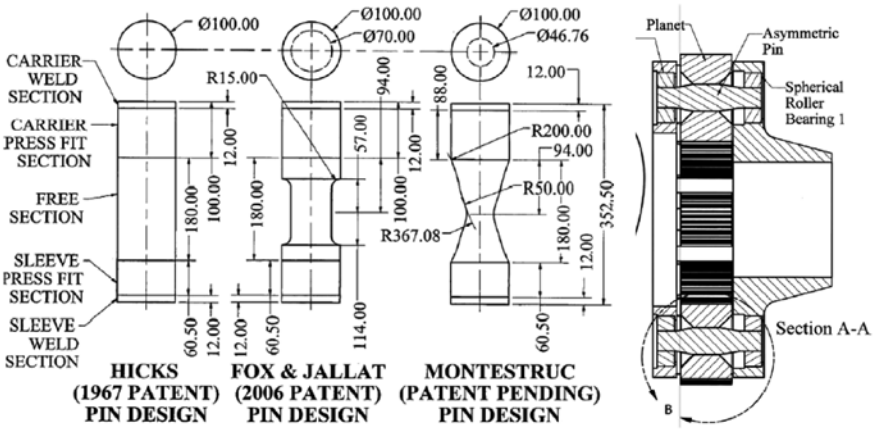

Figure 17—Different pin shapes compared (Ref. 6).

Shape Optimization

Based on the bending moment distribution along the pin, the required diameter at each point along the pin axis may be determined, resulting in an even stress level along the pin length (Ref. 20). Bending moment from left to right along the pin length is shown below.

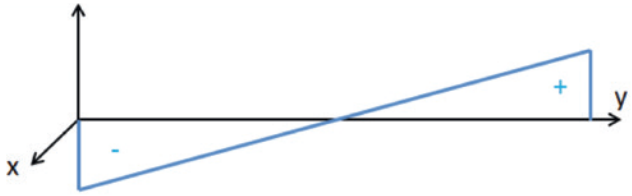

Figure 18—Bending moment over free length of Flexpin (vertical axis) vs. length / y-coordinate.

Bending moment, bending stress and required moment of resistance are then:

$$M_b(y) = F * \left(\frac{1}{2} - y\right), \sigma_{bzul} = \frac{M_b}{W_{erf}}, W_{erf} = \frac{M_b}{\sigma_{bzul}} \quad (1)$$

From this, the required pin diameter along the coordinate y can be calculated:

$$\frac{\pi * d_{erf}^3}{32} = \frac{F * \left(\frac{1}{2} - y\right)}{\sigma_{bzul}}, d_{erf}(y) = \sqrt[3]{\frac{32 * F * \left(\frac{1}{2} - y\right)}{\sigma_{bzul} * \pi}} \quad (2)$$

Note the above only considers bending moment. The resulting function, if plotted, gives a convex shape of the two halves of the pin, see below Figure, left:

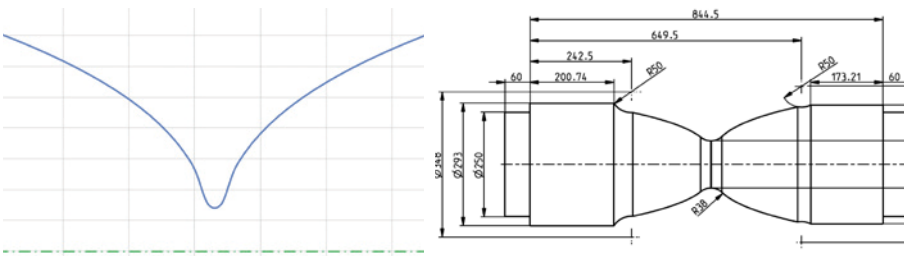

Figure 19—Resulting pin shape, considering bending stresses only, such that the stress level is constant along the pin length (note that in the middle, theoretically, the pin diameter would be zero).

The above shape (Figure 19, left), having a constant nominal bending stress along the longitudinal axis, serves as a basis for to design of the pin shape (Figure 19, right). In the middle of the pin, a cross-section is added such that the shear stress in the thin section is like the bending stress to the left and right. Furthermore, radii and relief grooves are incorporated, minimizing stress raisers. Analytical and FEM-based calculations are then used to confirm the even stress distribution below acceptable levels. Note that since the press fits between the pin of the Flexpin (2), on the lower left side of Figure 20, and the single-walled carrier (1) has a different stiffness than the one to the sleeve (3). Detailed FEM calculations showed that it is necessary to change the shape of the pin to an asymmetrical shape as shown in Figure 20, right.

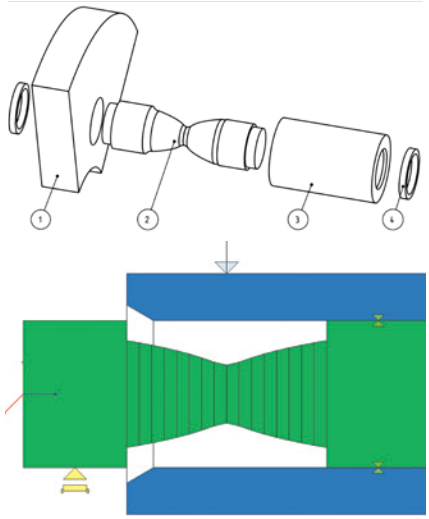

Figure 20—Top: Design with optimized pin (2) shape. Single-walled carrier (1) and sleeve (3). (Ref. 20). Bottom: Calculation model using two Timoshenko beams (green representing pin, blue representing sleeve). Press fit between pin and carrier and between pin and sleeve is by rigid connectors (yellow symbols).

Comparative Strength Assessment on Shape Optimized Flexpin Shapes

For a wind turbine of similar design as discussed above, now targeting 8 MW instead of 3 MW rated power, an initial design of a shape-optimized Flexpin of approximately 600 mm length was assessed. As the FEM analysis and stress assessment using gearbox torque time series is computationally expensive, a preliminary assessment using the nominal stress concept based on FKM guideline (Ref. 1) is used. FKM guideline method is preferred over DIN 743

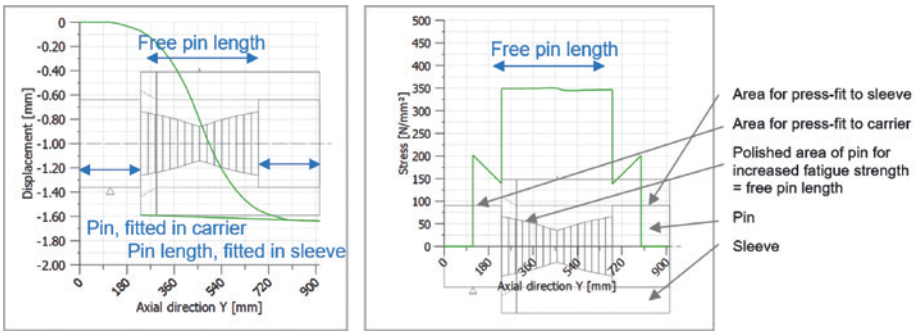

Figure 21—Left: Deformation. Right: Equivalent stress. Note: the nominal stresses (not considering notches/fillet radii) are now nearly constant along the free pin length.

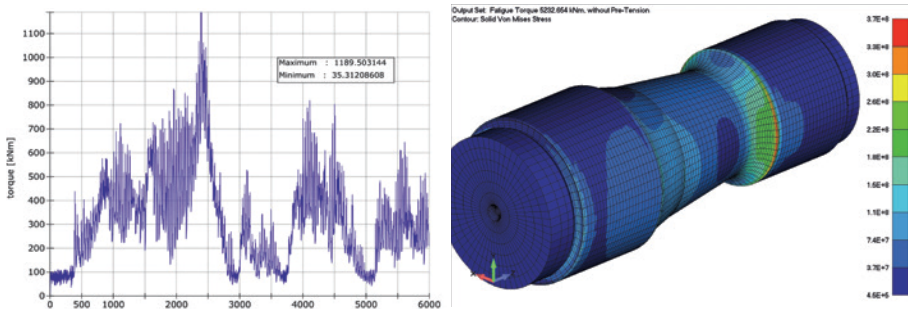

Figure 22—FEM based strength assessment of 3 MW MGB Flexpin. Left: Time series of torque used for fatigue rating of Flexpin. Right: Stress level in the pin at nominal torque.

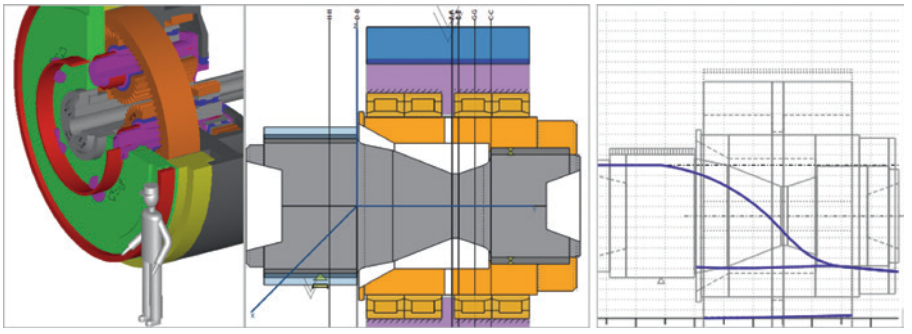

Figure 23—Left: 8 MW MGB model for analytical strength assessment. Middle: Flexpin model with optimized pin shape for comparative strength assessment. Right: Flexpin deformation (blue lines) based on Timoshenko beam model calculation, indicating that shape of Flexpin is suitable for keeping planet gears in parallel to gearbox axis under load.

(Ref. 2) here as the latter neglects shear stresses from shear forces which are relevant for short beams as present in the Flexpin pin. For this, the Flexpin design for which the FEM-based verification had been done and accepted by the certification agency along typical guidelines Refs. 3 and 4 earlier (for the 3 MW gearbox), were analyzed using FKM guidelines. In this, the rated torque, and a conservative assumption for the stress ratio (R=0) were used.

The resulting safety factors were then compared, and it was found that the Flexpin for the 8 MW gearbox displays slightly higher safety factors than the Flexpin for the 3 MW gearbox. In this, the technological and statistical size factors K_{dm} and K_{dp} are considered to account for the influence of larger part size for the 8 MW gearbox. Ultimate tensile strength at 1,250 MPa and yield strength at 1,050 MPa values were defined as target values in the manufacturing drawings and discussed with the forging company producing the forgings with a machining stock. The effect of the surface hardening by nitriding was neglected in the strength assessment as the part size was now such that the hardening depth achievable by nitriding was in the range of the depth of the stress concentration.

Conclusion

Flexpins are used in wind turbine MGB and other planetary gearboxes. It helps threefold:

- It improves the load sharing among the planets, in particular if the number of planets is higher than three. This is expressed in the gear rating with (a low) factor K_{γ}.
- It improves the load distribution along the gear face width. This is expressed in the gear rating with (a low) factor $K_{H\beta}$.
- It allows for the use of single-walled carriers where the planet pins are supported on one side only.

A low stiffness of the Flexpin is desirable to maximize the effect in the above points 1) and 2). While a thinner Flexpin pin results in lower stiffness, it also results in higher stresses. Optimizing the pin shape allows for a constant stress design, thereby maximizing the flexibility while keeping the stress levels within acceptable limits. As opposed to prior state-of-the-art, where cylindrical and other shapes are used, a parabolic shape, used in a symmetrical arrangement, is proposed here.

Furthermore, using simple spring models, the load-sharing factor K_{γ} may be predicted reasonably well. A gap–spring model was used to consider manufacturing and positioning errors along with component and gear mesh stiffness values. Numerical experiments using random error distributions were conducted and the 95-percentile value for K_{γ} was found at K_{γ_95} percent = 1.14. This was close to the value found in torque load test at $K_{\gamma\_torsion}$ = 1.12 yet still somewhat conservative. If in the test also bending loads were introduced, the K_{γ} value reached up to $K_{\gamma\_bending}$ = 1.23 which was still within the range defined by the value used in the gear design, as stipulated in design guideline (Ref. 3), at K_{γ_design} = 1.25.

As with respect to the design and manufacturing process of the Flexpin, experience has shown that:

- The use of a beam model for initial design of the Flexpin, in particular the pin, is sufficiently accurate for a preliminary design only.
- The beam model, where typically the pin is rigidly supported on

one side to represent its fit in the carrier and where the pin and the sleeve are typically rigidly connected to represent the fit between the two, is not accurate enough for a final design.

- FEM calculations considering the non-linear behavior of the press fits are required for design and verification of the final shape of the Flexpin and its deformation behavior.
- By introducing tilting stiffnesses in the beam model and tuning them such that the beam model yields similar deformation results as the FEM model, greatly improves the accuracy of the beam model. This lowers the number of FEM calculations needed to arrive at a final pin shape.
- Relief grooves in the pin lower stress concentrations induced by the press fits.
- Pin ultimate tensile and yield strength may be defined at 1,100–1,200 MPa to 900–1,000 MPa respectively. These levels may be achieved with commonly used steels such as 34CrNiMo6 and heat treatment applied after near-net shape machining.
- Nitriding, induction hardening, or case carburizing combined with polishing of the pin results in elevated part strength levels. The strength increase was assessed by introducing respective rating factors as per Ref. 1 and Ref. 2.
- The author has no experience with the shot peening of the Flexpin pin. Industry experience with similar parts proves the potential of the process.
- The press fits used were at 0.15 percent overlapping and proved to be working well in the field. No oil creep through the press fits was observed.
- A grinding or hard-turning operation to finalize the bearing seat after fitting the sleeve onto the pin is necessary.

The use of Flexpins in gearboxes allows for maximized torque density. Due to the higher material and manufacturing costs, it has not gained wide use. However, in gearboxes where the planet carrier only has one wall, it indeed solves the resulting issues elegantly.

Hanspeter Dinner joined KISSsoft AG in 2002 as a software support and project engineer. He has conducted about a hundred FEM, gear, bearings, and transmission projects serving the wind, tractor, industrial gearbox, and fine pitch gear industry. In his position as Deputy General Manager, he manages sales, support, trainings and engineering services teams of KISSsoft AG.

References

1. FKM-Guideline, Analytical Strength Assessment, 6th Edition.
2. DIN 743-1, 2, 3, Tragfähigkeitsberechnung von Wellen und Achsen.
3. Germanische Lloyd Rules and Guidelines Industrial Services, Guideline for the Certification of Wind Turbines, 2010.
4. ISO 81400-4:2005, Wind turbines, Part 4, Design and specifications of gearboxes.
5. Höller, A., Zumofen, L., Kirchheim, A., Dinner, H., & Dennig, H.-J. (2020). Additive manufactured and topology optimized Flexpin for planetary gears [Conference paper]. In M. Meboldt & C. Klahn (Eds.), Industrializing Additive Manufacturing : Proceedings of AMPA 2020 (pp. 337–356). Springer. *https://doi.org/10.1007/978-3-030-54334-1_24*
6. Montestruc, "Influence of Planet Pin Stiffness on Load Sharing in Planetary Gear Drives," *Journal of Mechanical Design*, 2011.
7. ANSI/AGMA 6123-C16, Design Manual for Enclosed Epicyclic Gear Drives.
8. NASA Technical Memorandum 107275, Effects of Planetary Gear Ratio on Mean Service Life.
9. Dinner et al., SCD SuperCompactDriveredesigned and sucessfullytested to meet floating offshore challenges, ATK & CWD 2019.
10. TIMKEN, Integrated Flexpin Bearing for Epicyclical Gearing Systems, The TIMKEN Company.
11. LaCava et al., Gearbox Reliability Collaborative: Test and Model Investigation of Sun Orbit and Planet Load Share in a Wind Turbine Gearbox, Conference Paper NREL/CP-5000-54618, April 2012.
12. Giger et al., High-Efficiency High Torque Gearbox for Multi Megawatt Wind Turbines, Scientific Proceedings VIII International Congress "Machines, Technologies, Materials" 2011.
13. Wang et al., Load Sharing Performance of Herringbone Planetary Gear System with Flexible Pin, International Journal of Precision Engineering and Manufacturing, 2019.
14. Tsai et al., Design and Analysis of the Planetary Gear Drive with Flexible Pins for Wind Turbines.
15. Giger, Planetenkoppelgetriebe in Windenergieanlagen mit flexibler Planetenlagerung, DMK 2003.
16. US Patent 3'303'713.
17. Raeber, R.; Weller, U.; and Amato, R., "A New Gearbox Generation for Vertical Roller Mills", Technical Paper, MAAG Gear AG, 2006.
18. *https://www.wikov.com/en/mechanical-gearboxes/according-to-application/wind-and-tidal, 19.5.2023*
19. *http://demo68.51-top.com/up/file/1/2018052821541263.png*
20. C. Röthlin, Flexpin Optimierung für die Anwendung in einer Multimegawatt Offshore Windturbine, Bachelor-Diplomarbeit in Konstruktion, Mechanik & Festigkeit, 2014.